Electric field effect on fast hydrogen atoms emerging from thin carbon foils

J. C. Dehaes and J. Carmeliet
Service de Métrologie Nucléaire (Code Postal 165), Université Libre de Bruxelles, 50 avenue F.D. Roosevelt, B-1050 Bruxelles, Belgium

H. G. Berry
Argonne National Laboratory, Argonne, Illinois 60439
(Received 19 June 1989)

When fast hydrogen atoms emerge from a thin carbon target, they interact with an electric field produced by the target itself. We have studied this interaction by measuring the total intensity and polarization of the Balmer lines as a function of the beam current. We have shown that the electric field increases with the beam current and acts over a distance of a few millimeters beyond the foil. A theoretical model has been developed. It reproduces the main features of the experimental data.

I. INTRODUCTION

The interaction processes occurring when a fast ion passes through a thin target have been studied for many years. It is by now well known that the excited atoms emerging from the target are aligned and also oriented if the target is tilted. Although there are many evidences of a large surface effect, the excitation mechanisms are not yet known. From a theoretical point of view, many attempts have been made to calculate the final density matrix describing the atomic excited states. The simplest model, i.e., the surface electric-field model proposed by Eck,[1] is only able to explain some aspects of the ion energy and target tilt-angle dependences.[2–6] More elaborate models based upon a microscopic description of the surface interaction are available (see Schröder and Gabriel[7] for a recent discussion of these models). Unfortunately these calculations cannot be made without a large number of approximations. This fact probably explains the discrepancies between the predictions of these models and the experiments. The observed beam current dependence of the beam-foil interaction makes the interpretation of the experiments more difficult. For helium, Gay and Berry[8] have proposed an explanation of this effect. It is based upon the interaction, at the exit surface, between the atoms and the secondary electron cloud. The physical process responsible for the current dependence of the secondary electron yield is not yet known, and a temperature effect seems to be unlikely.[9] For hydrogen, Singer *et al.*[10] have shown that the beam current effect is mainly due to the finite conductivity of the carbon foil. This model is supported by the measurements of the quantum beat pattern close to the foil which clearly shows the presence of an electric field extending over a distance of about 1 cm from the foil.[11] The Stark mixing induced by the electric field destroys almost completely the excitation state produced at the foil surface.

The purpose of this work is to make a more extensive study of this electric field and to compare the experimental results with model calculations. The measurements of the total intensity and polarization for the Balmer transitions from the $n=4$, 5, 6 and 7 levels were made for H^+ energies ranging from 50 to 100 keV.

II. EXPERIMENTAL METHOD

The experimental apparatus used at Argonne National Laboratory has been described elsewhere.[11] At Brussels, we used a 400-keV accelerator to produce a well-collimated H^+ beam. The target was a thin vacuum evaporated carbon foil (10 $\mu g\,cm^{-2}$) mounted on a single foil holder consisting of a large movable brass plate having a 7-mm-diam aperture. The target chamber was surrounded by two pairs of Helmholtz coils in order to reduce the magnetic field below 5 mG.

The light emitted by the foil-excited hydrogen atoms was detected at $90°\pm1°$ to the beam axis. The smallness of the solid angle made possible the measurement of the light emitted close to the foil without any significant vignetting effect. The length of the viewing region along the beam was defined by a one-to-one imaging of the beam on an adjustable slit. The detection system consists of a polarizer, an interference filter, and a cooled EMI-9502B photomultiplier with a dark count rate less than 2 counts/s. The pressure in the target chamber was maintained at about 10^{-6} Torr by a turbomolecular pump.

The light emitted by the hydrogen atoms emerging from a perpendicular foil is completely characterized by the intensities $I_{\parallel}$ and $I_{\perp}$ linearly polarized parallel and perpendicular to the beam axis. To determine these intensities, we first measured the number of counts normalized to a given charge collected at the screened Faraday cup and then, without the beam, the background counts during the same amount of time. We checked that the background due to the interaction of the beam with the residual gas was negligible.

III. THEORETICAL BACKGROUND

As usual, we have assumed that the beam-foil interaction is independent of the electronic spin. As a conse-

quence, the excitation state of a given n level at the exit surface of the foil can be described by a density matrix $\rho(0)$ in the (l,m) basis: $\langle l_1 m|\rho(0)|l_2 m\rangle$. This density matrix is diagonal in m because the z axis, aligned along the beam axis, is perpendicular to the foil.

For a Balmer transition in hydrogen, the zero-field total intensity $I_t=I_\parallel+2I_\perp$ and the polarization $M=I_\parallel-I_\perp$ are given by

$$I_t(t)=I_0\left[\rho_s e^{-\Gamma_s t}+(\rho_{p0}+2\rho_{p1})\frac{4(n^2-1)}{n^2}e^{-\Gamma_p t}+(\rho_{d0}+2\rho_{d1}+2\rho_{d2})\frac{32(n^2-1)}{5(n^2-4)}e^{-\Gamma_d t}\right], \tag{1}$$

$$M(t)=-I_0\left[(\rho_{p1}-\rho_{p0})\frac{4(n^2-1)}{n^2}\frac{1+2\cos(\omega_p t)}{3}e^{-\Gamma_p t}+(2\rho_{d2}-\rho_{d1}-\rho_{d0})\frac{16(n^2-1)}{5(n^2-4)}\frac{19+6\cos(\omega_d t)}{25}e^{-\Gamma_d t}\right.$$
$$\left.+|\rho_{sd}|8\left[\frac{n^2-1}{5(n^2-4)}\right]^{1/2}\left[\frac{2\cos(\omega_{3/2}t-\varphi_{sd})+3\cos(\omega_{5/2}t-\varphi_{sd})}{5}\right]e^{-(\Gamma_s+\Gamma_d)t/2}\right], \tag{2}$$

where $\tau_l=1/\Gamma_l$ is the lifetime of the l level and $I_0(n)$ is proportional to the Balmer transition probability. It is seen that the total intensity decays according to a multiexponential law, the amplitude of each exponential being proportional to the initial population of the corresponding l level: ρ_s, $\rho_{p0}+2\rho_{p1}$, $\rho_{d0}+2\rho_{d1}+2\rho_{d2}$. The polarization shows quantum beats whose amplitudes depend upon the alignment of the p and d states and upon the sd coherence $\langle s0|\rho(0)|d0\rangle=|\rho_{sd}|e^{i\varphi_{sd}}$. The beat frequencies are given by the fine-structure splittings: $\omega_p=\omega_{p3/2}-\omega_{p1/2}$, $\omega_d=\omega_{d5/2}-\omega_{d3/2}$, $\omega_{3/2}=\omega_{d3/2}-\omega_{s1/2}$, $\omega_{5/2}=\omega_{d5/2}-\omega_{s1/2}$. It is worth noting that the phases of the p and d beats are zero.

In the presence of an electric field, the density operator evolves according to

$$i\hbar\frac{\partial\rho}{\partial t}=[H,\rho], \tag{3}$$

where H is the sum of the free atom and external field Hamiltonians. Except in some particular cases, this equation cannot be solved analytically and the time dependence of I_t and M has to be calculated numerically.

The main effects of the electric field are that the total intensity is no longer a linear combination of three exponentials decaying with the s, p, and d lifetimes and that the quantum beat pattern changes drastically as we will see below. If, after it has interacted with the electric field, the hydrogen atom enters into a field free region the total intensity will recover a multiexponential decay, the amplitudes having changed due to the electric field. On the contrary, the expression of the polarization is no longer given by (2); the beat frequencies are, of course, the same but the amplitudes have changed and the phases of the p and d beats are no longer zero. As a consequence, there are two ways to detect an electric field close to the foil.

(i) Looking at the decay of the total intensity in the electric-field region. A departure from the "free-atom" decay is a very sensitive probe of the presence of an electric field.

(ii) Looking at the quantum beats in the field free region. The phases of the p and d beats must be zero if there is no electric field between the foil and the viewing region. It is also worth noting that the effect of the electric field increases with the principal quantum number n. Hence, by looking at transitions from a high-n level one can detect smaller electric fields.

IV. RESULTS

The anomalous decay of the total intensity is clearly seen in Fig. 1 which shows the first results obtained at Argonne for the Balmer transitions from the $n=6$, 7, 8, and 9 levels.[11] Up to 1 cm behind the foil, the total intensity exhibits an oscillation whose amplitude and shape change with n. For the $n=9$ level, the effect is so large that the s, p, and d levels are almost totally depopulated 2 mm downstream from the foil.

In Fig. 2 the results obtained at Brussels are shown. They confirm the previous results, i.e., the anomalous decay of I_t, and show that the total intensity is not maximum at the foil surface but is about 1 mm downstream. The total intensity for the $n=4$ level is only slightly disturbed while it decreases by a factor of 5 for the $n=7$ level with a lifetime of about 0.5 ns which is at least 100 times lower than the field-free lifetimes entering into Eq. (1). The sharp increase of the total intensity when the foil is moved out of the viewing region shows that the vignetting effect is small and that the foil could be located within ±0.1 mm. This allowed us to get a good estimate of the polarization close to the foil, i.e., the alignment induced only by the beam-foil interaction. As shown in Fig. 3, this initial polarization is small and obviously much lower than the amplitudes of the quantum beats observed downstream. There is an abrupt buildup of the polarization which is not compatible with Eq. (2).

These features may be summarized as follows:

(i) The polarization is positive and exhibits large quantum beats.

(ii) The beat phases are different from zero.

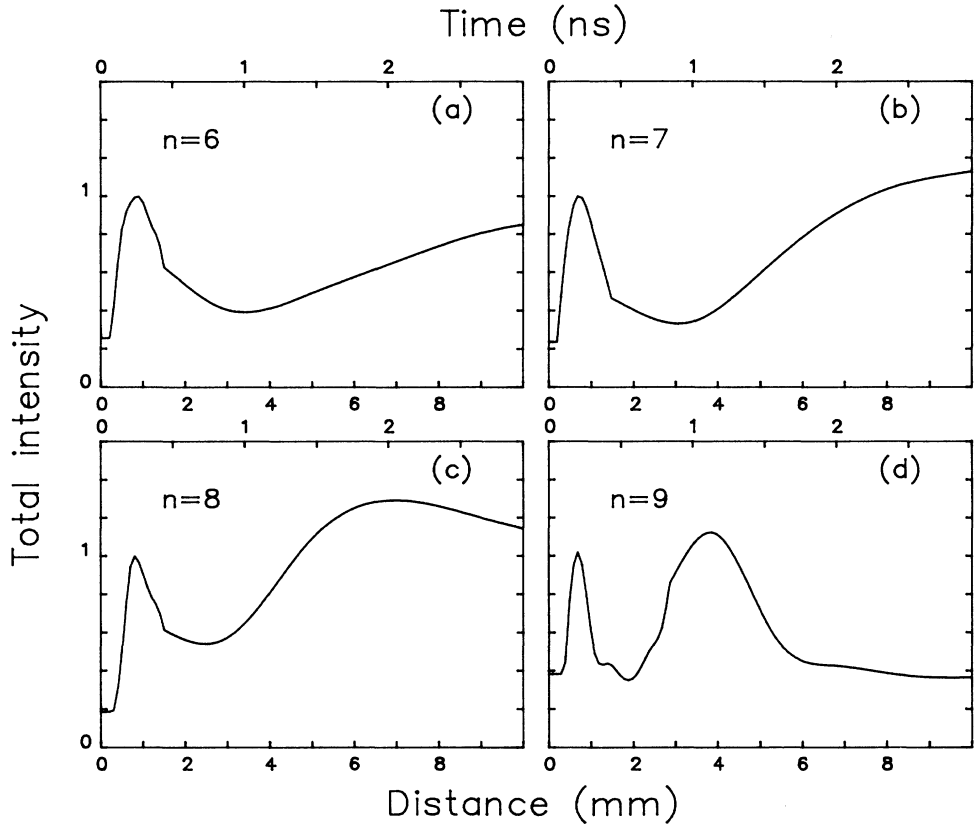

FIG. 1. Total intensity in arbitrary units as a function of distance from the foil for the Balmer transitions from the $n=6$ to 9 levels. In this experiment a 120-keV 15-μA H_2^+ beam and a double foil were used.

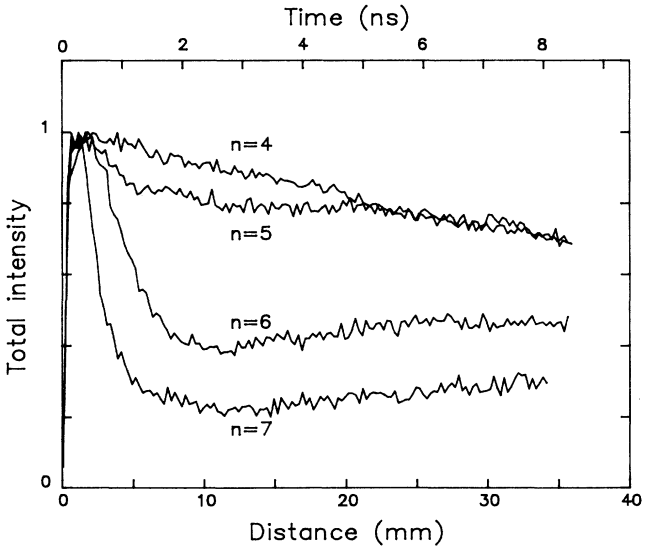

FIG. 2. Total intensity in arbitrary units as a function of distance from the foil for the Balmer transitions from the $n=4$ to 7 levels. In this experiment a 100-keV, 20-μA H^+ beam was used.

(iii) The maximum polarization increases with n, going from 0.1 for $n=4$ to 0.4 for $n=7$.

(iv) The polarization close to the foil is low.

This confirms the presence of an electric field and shows that most of the polarization, i.e., the atomic alignment, is induced by the electric field, the initial alignment being small. The experiments described below were done in order to show that the stray electric field is induced by the foil and depends upon the beam current.

A. Total intensity

In order to prove that the electric field is going to zero at low beam current, the total intensity decay should be measured as a function of beam current with the same foil. Unfortunately, the poor signal-to-noise ratio at low current makes this experiment unfeasible. Therefore, we measured the total intensities at 1 and 16 mm from the foil. Their ratio should be close to one if the electric field is zero. This experiment was done very carefully: using a small angular aperture of the light beam (1.7°), subtraction of background, repeated measurements alternatively at the two foil positions, and a homogeneous ion beam.

Typically results are given in Fig. 4. It is seen that the ratio of the total intensities are effectively close to one at

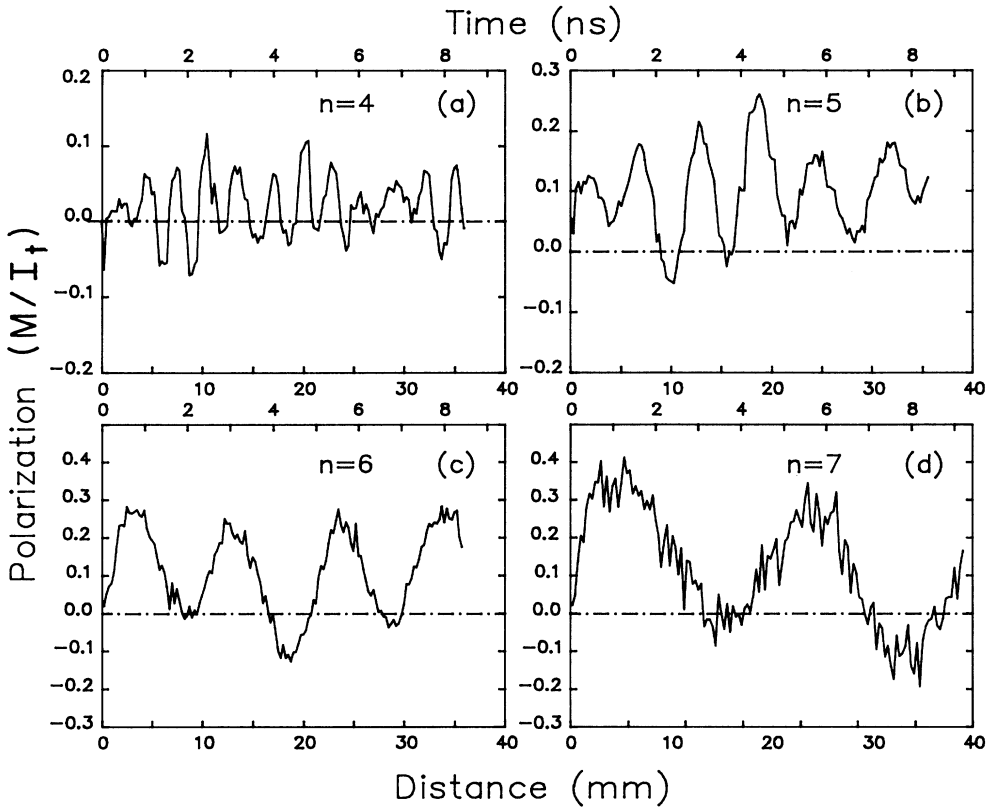

FIG. 3. Quantum beats on the linear polarization M/I_t for the Balmer transitions from the $n=4$ to 7 levels. These results were obtained with a 100-keV, 16-μA H^+ beam on a single foil.

low current and that the beam-current effect increases with n, as expected from the electric-field model. Figure 5 shows that the beam diameter plays almost no role but that the electric field changes when the foil diameter is changed. This result clearly shows that the observed effect is not a beam-current density effect. Indeed, at a given current, the measured ratio doesn't depend upon the beam diameter and decreases when the foil diameter is smaller. From these experiments, we conclude that the electric field is a function of the beam current which de-

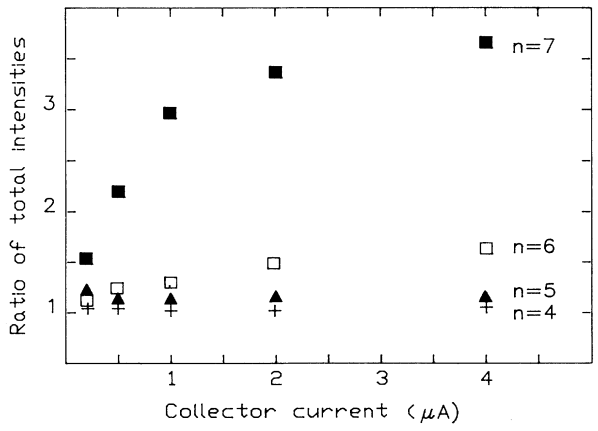

FIG. 4. Ratio of the total intensities measured at 1 and 16 mm behind the foil as a function of the current collected at the Faraday cup. The energy of the H^+ beam is 100 keV.

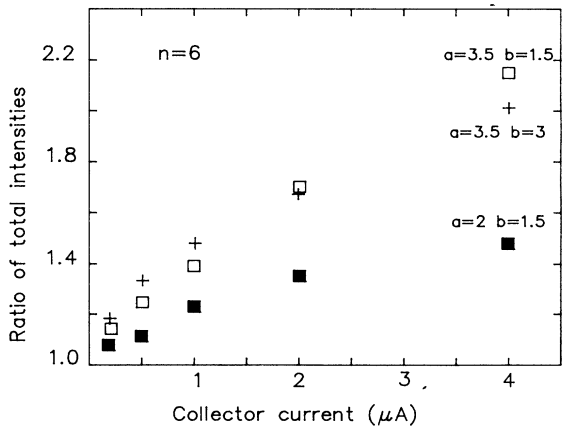

FIG. 5. Ratio of the total intensities measured at 1 and 16 mm behind the foil as a function of the current collected at the Faraday cup. The length of the viewing region is 1 mm wide and the energy of the H^+ beam is 75 keV, a is the beam radius and b the foil radius in millimeters.

creases to zero at low current. Furthermore, the amplitude and shape of this electric field must give rise to a final effect which increases with the foil diameter.

B. Linear polarization

The linear polarization was measured at 1 mm from the foil and with a slit width equal to 1 mm using the same experimental procedure as for the total intensity measurements. The beam-current dependence of the relative polarization close to the foil is shown in Fig. 6. It is seen that M/I_t is a strong function of beam current and that it is close to zero and even negative at low current. It must be emphasized that these measurements are very sensitive to the length the viewing region along the beam because of the sudden rise of the polarization induced by the electric field (see Fig. 3). These results support the already mentioned conclusion that the positive polarization is produced by the electric field and not by the target. It is also interesting to notice that the polarization extrapolated to zero current is independent of n within the experimental errors and approximately equal to 0 at 50 keV, -0.015 at 75 keV, and -0.04 at 100 keV.

Figure 6(d) shows that the linear polarization depends only upon the foil diameter and not upon the beam diameter. This measurement done at 1 mm behind the foil confirms the same feature observed on the total intensity measured at 16 mm.

C. Conclusions from the experiments

Two kinds of conclusions can be drawn. First, the electric field is produced by the beam and it depends upon the beam current. Very low currents are required, less than 0.1 μA for $n=7$, to avoid any significant field effect. The perturbation induced by this field is not a function of the beam diameter, and hence it is not a beam-current density effect. This field acts over a distance of about 2–3 times the foil radius. On the other hand, the large atomic alignment is produced by the field, while the alignment at the foil surface is small and negative above 50 keV, as already observed for the $n=2$ level[12,13] and the $n=3,4$ levels.[14,15]

V. MODEL CALCULATIONS

In order to calculate the total intensity and polarization, we have to solve the evolution equation (3) for the density matrix with a Hamiltonian which includes the electric field. The main problem is that neither the initial density matrix nor the shape and amplitude of the electric field are known.

Furthermore, the number of independent density matrix elements is given by $n(n+1)(2n+1)/6$ if spin independence and axial symmetry are assumed. This number of unknowns can be very large, even for low n: 30 for $n=4$, 55 for $n=5$, and 91 for $n=6$.

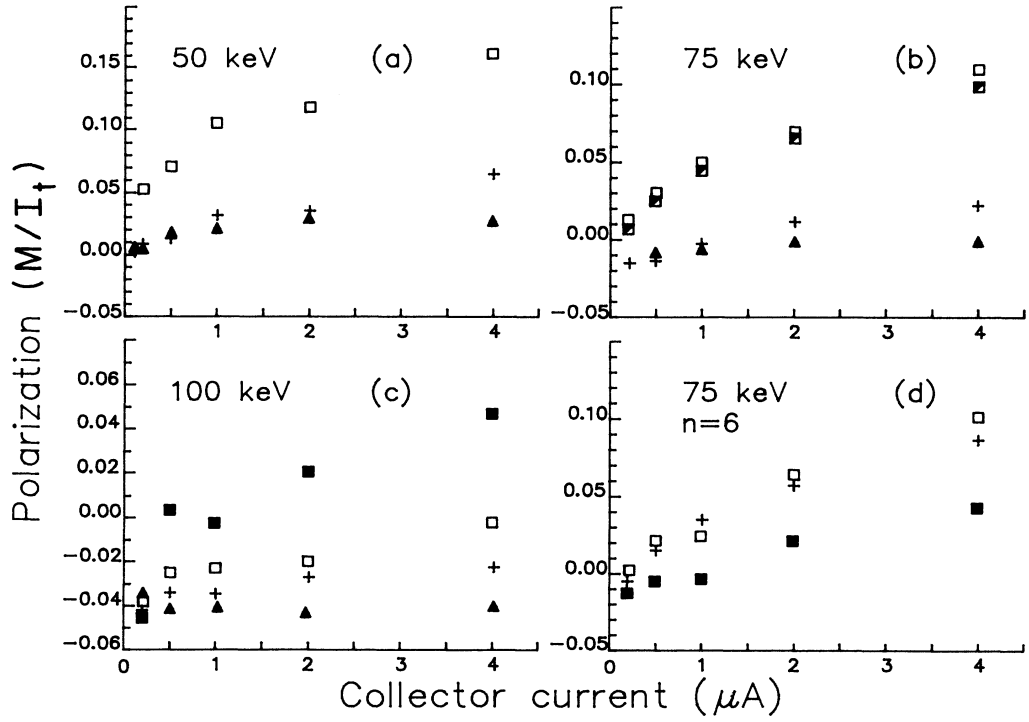

FIG. 6. Linear polarization M/I_t measured 1 mm behind the foil as a function of the current collected at the Faraday cup. For the meaning of the symbols, see Figs. 4(a)–4(c) and Fig. 5(d). The standard error is less than 0.005.

The electric field is axially symmetric for a perpendicular foil, hence in cylindrical coordinates it is a function of r and $z = vt$, where v is the velocity of the atoms. As a result, the density matrix must be calculated as a function of z (or t) for each r in order to calculate the average density matrix $\langle \rho \rangle = \int_0^b \rho(r) 2\pi r \, dr$, where b is the beam radius.

It is obvious that it would not be fruitful to use a fitting procedure in order to obtain the initial density matrix and the electric field from the experimental data. Hence we choose to make very simple but realistic assumptions to search for agreement with the experimental results.

A. Initial density matrix

We assumed that all the off-diagonal density matrix elements are equal to zero, i.e., the even and odd coherences are ignored. Hence we have to choose $n(n+1)/2$ matrix elements $\rho_{lm} \equiv \langle lm | \rho(0) | lm \rangle$ which are the populations of the (l,m) levels. If the levels are statistically populated, i.e., $\rho_{lm} = 1$, then the electric field has a negligible effect and the total intensity and polarization remain almost undisturbed. Our choice was based upon the experimental observation that the polarization close to the foil is small ($-0.04 < M/I_t < 0$). As a result, the population ρ_{lm}, for a given l level, should not depend too much on m. The simplest choice is then $\rho_{lm} = 1/2l+1$, i.e., a uniform population of the l levels.

Other population distributions have been checked.

(i) Only the s state populated.
(ii) Only high l levels populated.
(iii) Only $m = 0$ levels populated.

In all these cases, we found a disagreement with the experimental data either in the total intensity decay or in the quantum beat pattern. It must be emphasized that a uniform population of the l levels has been chosen for convenience and that there are many other population distributions which can also give a good agreement with the experimental results.

B. Electric field

For simplicity, the calculations were done using the calculated electric field along the beam axis, where it is longitudinal. As a consequence, we ignored the radial component and the fact that the longitudinal component is a function of r. This axial field $E_z(z)$ was calculated in three cases.

(i) A uniform charge distribution σ_0 on the foil surface,

$$E_z(z) = \frac{\sigma_0}{2\epsilon_0} \left[1 - \frac{(z/a)}{(1+(z/a)^2)^{1/2}} \right] . \tag{4}$$

(ii) A uniform potential distribution V_0 on the foil surface,

$$E_z(z) = \frac{V_0}{a} \left[\frac{1}{[1+(z/a)^2]^{3/2}} \right] . \tag{5}$$

(iii) A potential distribution taken from the "foil resistance model"[10]

$$E_z(z) = \frac{2V_0}{a} \left[\left[\frac{1+2(z/a)^2}{(1+(z/a)^2)^{1/2}} \right] - 2z/a \right] , \tag{6}$$

where a is the radius of the charge or potential distribution.

Figure 7 compares the z dependences of the electric potential and field for a unit potential at the center of the foil. The parabolic potential distribution gives rise to the highest electric field close to the target but it decreases much faster than those generated by the other potentials. For a uniform charge or potential distribution, the electric field extends over a much greater distance. This feature is important because the experiments have shown that the electric field acts over a distance of the order of one foil diameter.

C. Numerical calculation of the total intensity and polarization

In order to compute the time dependence of the total intensity and polarization for a Balmer transition, we have developed a program which solves Eq. (3) for the density matrix elements. It assumes that the electric field is aligned along the foil normal and that the initial density matrix for a given hydrogenic n level is diagonal in m,

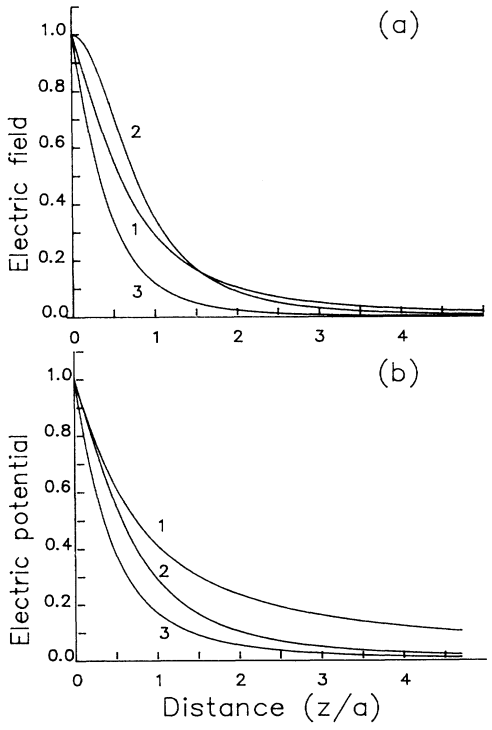

FIG. 7. (a) Longitudinal electric field and (b) electric potential along the beam axis: 1, uniform charge distribution on the foil surface; 2, uniform potential distribution on the foil surface; 3, parabolic potential distribution on the foil surface (the electric field has been divided by 2).

i.e., the interaction with the foil and with the electric field is axially symmetric. The Hamiltonian is the sum of the free-atom Hamiltonian, including the precise energy and lifetime of each sublevel, and of the Stark Hamiltonian. The matrix elements are calculated in the LS coupling scheme using hydrogenic wave functions. They are linear in the electric field because the coupling between different n levels has been ignored. Instead of directly solving Eq. (3), we found it more convenient to solve the equation for the evolution operator $U(t)$ from which we can obtain the density operator using the well-known relation $\rho(t)=U^{\dagger}(t)\rho(0)U(t)$. The evolution operator has been calculated at equally spaced values of t, and it has been assumed that it can be approximated by

$$\exp\left[-\frac{i}{\hbar}\int_{t}^{t+\Delta t}H(t)dt\right].$$

To calculate this exponential, we have used the second degree diagonal Padé approximation which, in our case, seems to give a good compromise between accuracy and speed. All the calculations have been done on the CYBER 180 of the Université Libre de Bruxelles computer center.

D. Theoretical results

Although the calculations have been done for the $n=3$ to 6 levels, we will only show the results obtained for the Balmer transition from the $n=6$ level at a proton energy of 75 keV and assuming an uniform initial population of the l sublevels. The comparison with the experimental results has been done by varying the following.

(i) The kind of potential or charge distribution on the foil surface whose radius is a. This defines the z dependence of the electric field and potential.

(ii) The value of the electric potential V_0 at the center of the foil.

The results shown in Fig. 8 have been obtained for $V_0=7$ V and $a=3.5$ mm, which corresponds to an electric field at $z=0$ of 20 V/cm for the uniform charge and potential distribution and 40 V/cm for the parabolic potential distribution.

It is seen that the observed initial increase of the total intensity can be reproduced and that its slope depends upon the amplitude of the electric field. At larger distances, the total intensity decays more or less proportionally to the electric potential and eventually it decays according to Eq. (1). It is worth noting that, in the field-free region, the total intensity is almost only sensitive to the value of V_0 and not upon the way the potential decreases to zero. Calculations done as a function of energy have shown that the important parameter is V_0/v, where v is the velocity of the atom.

The same features are seen on the quantum beats superimposed on the linear polarization: the initial increase depends upon the electric field while the zero-field quantum beats are more sensitive to the potential. The same figure shows also that it is the electric field which produces the large positive polarization at about 2 mm from the target.

These results reproduce rather well the experimental data shown in Figs. 2 and 3. The shapes of the measured and calculated total intensities are qualitatively the same and the phase and amplitude of the quantum beats are almost exactly the same as those which have been measured.

These comparisons suggest that the potential induced by a 100-keV, 20-μA H^+ beam impinging on a 10-$\mu g\,cm^{-2}$ carbon foil is about 10 V. By comparing the shapes of the decay of the total intensity and the phases of the quantum beats, we may conclude that the best agreement is obtained from a uniform charge distribution. Figure 9 shows how the total intensity changes with V_0. At $V_0=17.5$ V, the total intensity is in good agreement with the experimental results (see Fig. 1) obtained at Argonne with a 120-keV, 15-μA H_2^+ beam. Assuming that V_0 is proportional to the beam current, we can calculate $V_0/(vI_b)$ at 60 and 100 keV: there is a factor of 2 between the Argonne and Brussels experiments. Differences in the experimental setup, especially in the

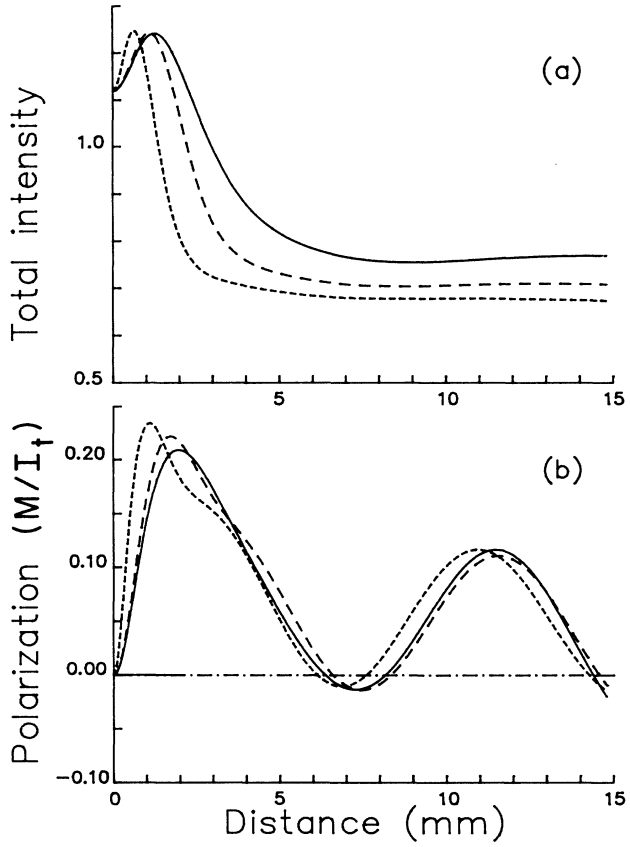

FIG. 8. Calculated time dependence of (a) the total intensity and (b) the polarization for the $n=2$ to $n=6$ Balmer transition for $a=3.5$ mm and a 75-keV H^+ beam. The potential at the foil surface is 7 V. ——, uniform charge distribution; — — —, uniform potential distribution; — — —, parabolic potential distribution.

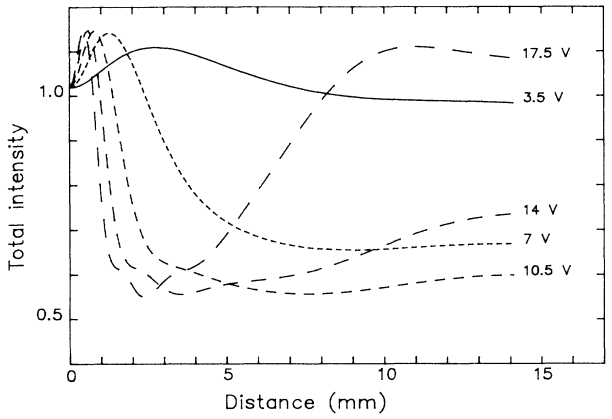

FIG. 9. Calculated decay of the total intensity for the $n=2$ to $n=6$ Balmer transition for $a=3.5$ mm and a 75-keV H^+ beam. The potential at the foil surface varies from 3.5 to 17.5 V.

close environment of the target, are probably responsible for this discrepancy.

The dependence of the total intensity upon the radius of a uniform charge distribution is shown in Fig. 10. For a given electric field at the center of the foil, the perturbation induced on the decay of the total intensity increases with the radius a, but at distances larger than 5 mm the total intensity is mostly sensitive to $V_0=E_0a$. Applying this conclusion to the experimental results (see Fig. 5), we find that V_0 increases with the beam current (at least for $I_b<7$ μA) as expected, and that it increases with the foil radius. The same trends can be deduced from the linear polarization.

VI. CONCLUSIONS

We have shown experimentally that a hydrogen atom emerging from a thin carbon target is perturbed by an electric field which acts over a distance of several millimeters beyond the foil. The amplitude of this electric field increases with the beam current. This effect has been observed in both the decay of the total light yield and in the polarization of the Balmer lines of the excited states of principal quantum number $n=4$ up to $n=8$. Even low currents (of about 0.1 μA) give rise to a significant effect on the $n\geq 6$ levels. Hence, the study of any *foil-induced excitation* effects on such levels is very difficult: minimizing electric-field effects by use of low-beam currents yields large statistical errors in the data.

We also show that the large positive polarization observed close to the foil is due entirely to this electric field,

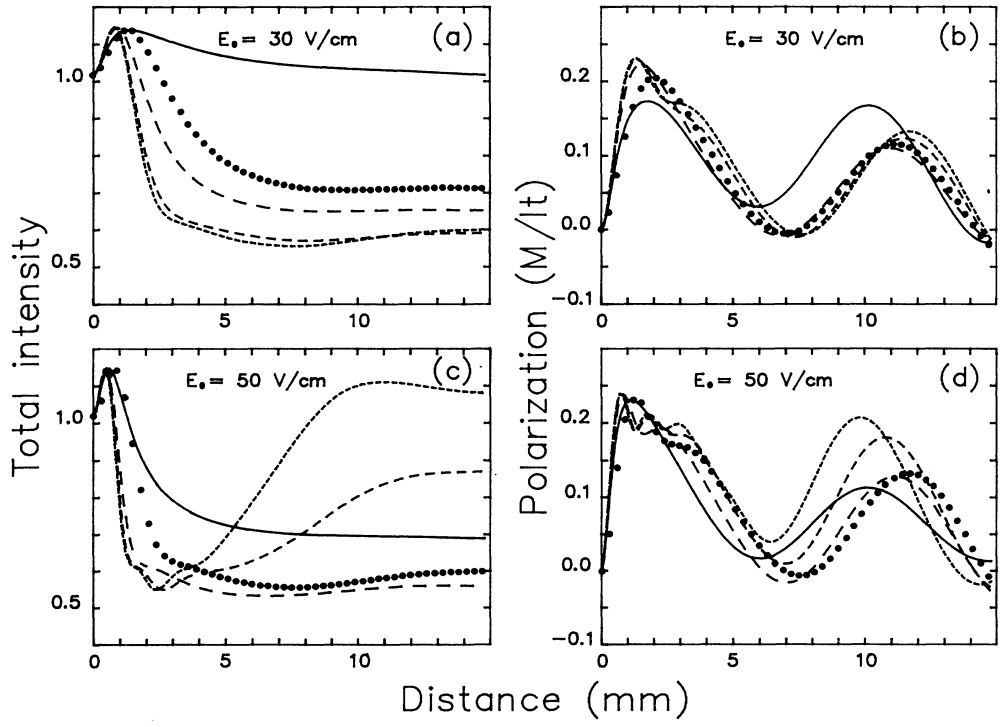

FIG. 10. Calculated time dependence of the total intensity for the $n=2$ to $n=6$ Balmer transition for and a 75-keV H^+ beam. ——, $a=3.5$ mm; –, $a=3$ mm; — — —, $a=2$ mm; ———, $a=1$ mm; · · · ·, (a) and (b), $a=3$ mm and $E_0=20$ V/cm, (c) and (d), $a=3.5$ mm and $E_0=30$ V/cm.

the polarization extrapolated to zero current near the foil surface is found to be small and negative. This is in agreement with other results on the polarizations measured for transitions from lower n levels ($n=2$[12,13], $n=3$[14], $n=4$,[14,15] at generally higher beam energies. For this lower n levels, the electric-field effects are most negligible, as is shown from our data for $n=4$.

We have calculated the time evolution of the total intensity and polarization of light emitted by an excited hydrogen atom traversing an electric field. We obtain good agreement with the measured results when we assume that the l levels are equally populated, and that the electric field is produced by a uniform potential or a uniform charge distribution on the foil surface. Although this model seems physically reasonable, and gives good agreement with the data, it may not be a unique solution. However, other similar population distributions give markedly different results.

The finite conductivity of the carbon foil is probably responsible for the electric field. However, we do not understand the variation of the electric-field strength that is observed as a function of the foil diameter. We would expect that the conductivity model would lead to small field strengths for large foil diameters, but our results show the opposite effect (Fig. 5). The electric field is independent of the beam-current density for a given beam diameter, but increases at larger foil diameters for a fixed beam current and beam current density. Hence, our remaining problem is the question of the formation of the surface electric field. This must be closely tied to the secondary electron production, since low-energy electrons will be trapped in the surface field, and return to the surface setting up an equilibrium field which is clearly different for different foil geometries. Thus, although qualitatively, the results from Argonne and Brussels agree, the differences can be attributed to these geometrical differences. The slow-electron trajectories may also be strongly affected by the beam and foil diameters for the different geometries (see, e.g., Singer *et al.*[10]). These uncertain variations may be responsible for these two unexpected results. Further work is clearly necessary to complete the analysis of the surface field production mechanisms.

ACKNOWLEDGMENTS

This work was supported in part by a NATO grant, the Institut Interuniversitaire des Sciences Nucléaires (IISN), and the U.S. Department of Energy.

[1]T. G. Eck, Phys. Rev. Lett. **33**, 1055 (1974).
[2]Y. B. Band, Phys. Rev. A **13**, 2061 (1976).
[3]J. C. Dehaes, M. Schenkel, and J. Devooght, Nucl. Instrum. Methods **202**, 235 (1982).
[4]J. C. Dehaes and J. Carmeliet, J. Phys. B **17**, 3029 (1984).
[5]T. J. Gay, H. G. Berry, R. DeSerio, H. P. Garnir, R. M. Schectman, N. Schaffel, R. D. Hight, and D. J. Burns, Phys. Rev. A **23**, 1745 (1981).
[6]R. M. Schectman, R. D. Hight, S. T. Chen, L. J. Curtis, H. G. Berry, T. J. Gay, and R. Deserio, Phys. Rev. A **22**, 1591 (1980).
[7]H. Schröder and H. Gabriel, Nucl. Instrum. Methods, B **24/25**, 291 (1987).
[8]T. J. Gay and H. G. Berry, Phys. Rev. A **19**, 952 (1979).
[9]J. C. Dehaes, J. Carmeliet, and A. Dubus, Nucl. Instrum. Methods B **13**, 627 (1986).
[10]W. Singer, J. C. Dehaes, and J. Carmeliet, Phys. Scr. **21**, 165 (1980).
[11]H. G. Berry, J. C. Dehaes, D. K. Neek, and L. P. Somerville, *Forward Electron Ejection in Ion Collisions,* Vol. 213 of *Lecture Notes in Physics,* edited by K. O. Groeneveld, W. Meckbach, and I. A. Sellin (Springer-Verlag, New York, 1984), p. 150.
[12]H. Winter and H. H. Bukow, Z. Phys. A **277**, 27 (1979).
[13]G. Gabrielse, Phys. Rev. A **23**, 775 (1981).
[14]A. Denis, J. Desesquelles, M. Druetta, and M. Dufay, in *Beam Foil Spectroscopy,* edited by I. A. Sellin and D. J. Pegg (Plenum, New York, 1976), p. 799.
[15]J. Carmeliet, J. C. Dehaes and W. Singer, J. Phys. Paris Colloq. **40**, C1-335 (1979).